Available online at www.sciencedirect.com

SciVerse ScienceDirect

Ceramics International 39 (2013) 1723–1728

CERAMICS INTERNATIONAL

www.elsevier.com/locate/ceramint

Synthesis and luminescence properties of novel $LiSr_4(BO_3)_3:Dy^{3+}$ phosphors

Zhi-Wei Zhang[a,*], Xin-Yuan Sun[b], Lu Liu[a], You-shun Peng[a], Xi-hai Shen[a], Wei-Guo Zhang[a], Dong-Jun Wang[a]

[a]*Physical-Chemistry College, Hebei Normal University of Science and Technology, Qinhuangdao 066604, PR China*
[b]*Department of Physics, Jinggangshan University, Ji'an 343009, PR China*

Received 7 August 2012; accepted 8 August 2012
Available online 18 August 2012

Abstract

The $LiSr_4(BO_3)_3:Dy^{3+}$ phosphors were synthesized in air by solid-state reaction route. The as-synthesized phosphors were characterized by X-ray powder diffraction (XRD), photoluminescence excitation (PLE) and photoluminescence (PL) spectra. The PLE spectra show the excitation peaks from 300 to 400 nm is due to the *4f–4f* transitions of Dy^{3+}. This mercury-free excitation is useful for solid state lighting and light-emitting diodes (LEDs). The emission of Dy^{3+} ions upon 350 nm excitation is observed at 481 nm (blue) due to the $^4F_{9/2}\rightarrow{}^6H_{15/2}$ transitions, and 575 nm (yellow) due to $^4F_{9/2}\rightarrow{}^6H_{13/2}$ transitions. The optimal PL intensity of the $LiSr_4(BO_3)_3:Dy^{3+}$ phosphors under 350 nm excitation is found to be at the concentration of $x=0.02$ and the synthesis temperature at 1000 °C. The CIE chromaticity coordinates for $LiSr_4(BO_3)_3:Dy^{3+}$ phosphors are simulated and located in the bluish-white region. All the results imply that the studied $LiSr_4(BO_3)_3:Dy^{3+}$ phosphors could be potentially used as white LEDs.

Keywords: Solid-state reaction; $LiSr_4(BO_3)_3:Dy^{3+}$ phosphors; Photoluminescence; White LEDs

1. Introduction

White light-emitting diodes (w-LEDs) are the promising new emitting light source for common illumination because of their unique properties in terms of low energy consumption, long lifetime and environment friendliness [1–3]. White light emission resulted from a single-phase phosphor is expected to obtain high luminous efficacy in comparison with that from two or three phosphors, because it could avoid multi-phosphors re-absorption of emission colors. Therefore, single phase white-emitting phosphors are required for UV-pumped w-LEDs to improve the luminescence reproducibility and efficiency [4–7].

Phosphors are usually made from a suitable host material, to which an idea activator is incorporated to get the designed emission peaks or bands. The well used host materials are aluminates [8], phosphates [9], silicates [10] and borates [11–13]. Among them, the borate-based phosphors such as $Ca_3Y(GaO)_3(BO_3)_4:Ce^{3+}$, Mn^{2+}, Tb^{3+} [11], $Ba_2LiB_5O_{10}:Dy^{3+}$ [12] and $Sr_3RE_2(BO_3)_4:Dy^{3+}$ [13], due to their excellent thermal stability, environmental benignity and potential low-cost synthesis, have attracted extensive attention. In recent years, the $MM'_4(BO_3)_3$ (M=Li, Na, K; M'=Ca, Sr, Ba) borate host doped with rare earths deserve more concentration on its luminescent properties. Wu and his coworkers have reported and studied photoluminescence of samples doped with the ions Eu^{2+} and Eu^{3+} for the first time [14]. After then, a series of novel rare dopped borates, $MM'_4(BO_3)_3$ phosphors have been successfully synthesized, such as $NaSr_4(BO_3)_3:Ce^{3+}$, Tb^{3+} [15], $LiSr_4(BO_3)_3:Ce^{3+}$ [16], $NaCa_4(BO_3)_3:Eu^{3+}$ [17], $NaSr_4(BO_3)_3:Ce^{3+}$, Eu^{3+}, Tb^{3+} [18]. These materials emit intense visible light and are promising phosphors for practical application. However, the PL

*Corresponding author. Tel.: +86 335 2039067.
E-mail address: zhangzhiweia@163.com (Z.-W. Zhang).

0272-8842/$ - see front matter © 2012 Elsevier Ltd and Techna Group S.r.l. All rights reserved.
http://dx.doi.org/10.1016/j.ceramint.2012.08.017

properties of these materials have not been investigated widely. This prompted us to study the fluorescence properties of rare earth ions in these borates.

Rare earth Dy^{3+} ions have two dominant emission bands in the blue region (470–500 nm) due to $^4F_{9/2}$–$^6H_{15/2}$ transition and in the yellow region (560–600 nm) due to $^4F_{9/2}$–$^6H_{13/2}$ transition. It is possible to achieve near white light emission by adjusting the yellow to blue intensity ratio value. Consequently, Dy^{3+}-activated luminescent materials attracted much attention [19,20] because of their significant applications as potential single phase white phosphors. To our best knowledge, the luminescence properties of $LiSr_4(BO_3)_3$:Dy^{3+} phosphor have hardly been reported. In this paper, $LiSr_4(BO_3)_3$:Dy^{3+} phosphors were synthesized successfully by the solid-state reaction. The corresponding structure and luminescent properties were characterized by XRD and PL spectra. The simulated CIE of $LiSr_4(BO_3)_3$:Dy^{3+} phosphors were also calculated. The results suggest that $LiSr_4(BO_3)_3$:Dy^{3+} might be used as a potential single phase phosphor for NUV-based w-LEDs.

2. Experimental

Powder samples with stoichiometric composition of $LiSr_{4-x}(BO_3)_3$:xDy^{3+} ($x=0.0$, 0.005, 0.01, 0.015, 0.02, 0.03 and 0.06) phosphors were synthesized by high temperature solid-state route. Raw materials of $SrCO_3$, H_3BO_3, Li_2CO_3 (Shanghai Chemical Reagent, A.R. grade) and Dy_2O_3 (Shanghai Yuelong New Materials Co. Ltd., 99.99%) were mixed thoroughly in an agate mortar. The amount of H_3BO_3 was excess of 5% to compensate its evaporation losses during the synthesis process. The well-ground mixtures were calcined in the 850 °C–1050 °C temperature range with a interval step of 50 °C for 300 min in air, then cool down naturally to room temperature. The synthesis reaction could be described as follows:

$$Li_2CO_3+6H_3BO_3+(8-2x)SrCO_3+\frac{x}{2}+Dy_2O_3\rightarrow 2LiSr_{4-x}(BO_3):xDy^{3+}+(9-2x)CO_2+9H_2O$$

The phase purity of the as-synthesized phosphors was investigated by X-ray powder diffraction spectroscopy (XRD) with a X-ray Diffractometer (Brucker D8) with Cu-Ka radiation at 40 kV and 40 mA. The XRD patterns were collected in the range of $10^\circ \le 2\theta \le 80^\circ$. The PL and PLE spectra were recorded on a Hitachi F-7000 fluorescence spectrometer with a 150 W-xenon lamp. All the measurements were carried out at room temperature.

3. Results and discussion

3.1. Crystal structure

As shown in Fig. 1, $LiSr_4(BO_3)_3$ crystallizes in the cubic space group $Ia\bar{3}d$ with large lattice parameters:

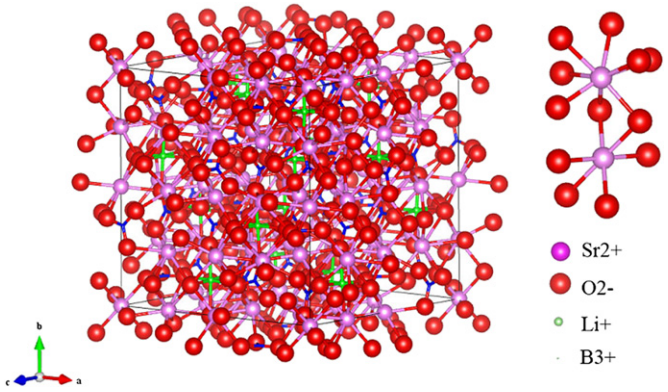

Fig. 1. Crystal structure of $LiSr_4(BO3)_3$.

$a=14.95066(5)$ Å and $V(cell\ volume)=3341.80(2)$ Å^3. The structure is constructed by 64 small cubic grids. The Sr atoms take up the corner angle and three interperpendicular BO_3 groups and LiO_6 cubic octahedra alternately fill in the interspaces of the cubic grids. The anisotropic polarizations were counteracting, forming an isotropic crystal. In the crystal structure of $LiSr_4(BO_3)_3$, there are two different crystallographic sites for Sr atoms in the $LiSr_4(BO_3)_3$ compound. The Sr(I) atom is coordinated to six oxygen atoms, forming a distorted octahedron, and it is centrosymmetric (16a); while the Sr(II) atom is eight-coordinated to oxygen atoms, forming a $Sr(II)O_8$ polyhedron, and it is noncentrosymmetric (48f) [14,21]. It is well known that an acceptable percentage difference in ion radii between the doped and substituted ions must not exceed 30%, which suggests that Dy^{3+} ions (1.027 Å) may prefer to substitute Sr^{2+} (1.260 Å) cation ions rather than Li^+ (0.059 Å) [22]. Therefore, the general formula of the investigated phosphors is described as $LiSr_{4-x}(BO_3)_3$:xDy^{3+}, where x denoting the substitution ratio of Dy^{3+} for Sr^{2+} ions.

3.2. Luminescence properties for $LiSr_4(BO_3)_3$:Dy^{3+} phosphors at different synthesis temperature

3.2.1. XRD analysis

The $LiSr_{3.98}(BO_3)_3$:$0.02Dy^{3+}$ powders were prepared by high temperature solid state reaction method and calcined in the 850 °C–1050 °C temperature range with an interval step of 50 °C. Fig. 2 shows the XRD patterns for $LiSr_{3.98}(BO_3)_3$:$0.02Dy^{3+}$ powders at different temperatures. As shown in Fig. 2, the $LiSr_{3.98}(BO_3)_3$:$0.02Dy^{3+}$ powders have several diffraction peaks, which are in almost agreement with that of the JCPDS 17–0861 card for $LiSr_4(BO_3)_3$ [14]. Besides, a small amount impurity phases of $Sr_3B_2O_6$ (JCPDS 35–0144) [23] existed in the XRD patterns. The main sharp peak suggests that the structure of the crystalloid is well crystallized, which imply that the $LiSr_{3.98}(BO_3)_3$:$0.02Dy^{3+}$ phosphors have been successfully prepared. Moreover, the incorporation of Dy^{3+} ions did not change the single-phase structure of $LiSr_4(BO_3)_3$ due to the low dopant concentrations.

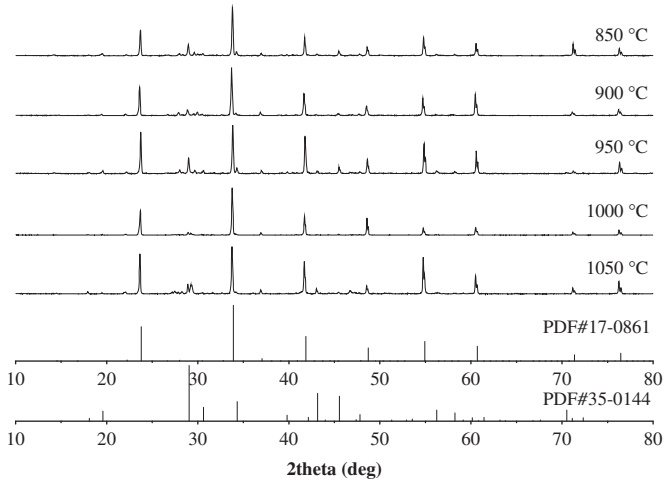

Fig. 2. XRD patterns for $LiSr_{3.98}(BO_3)_3$:0.02Dy^{3+} powders at different temperatures.

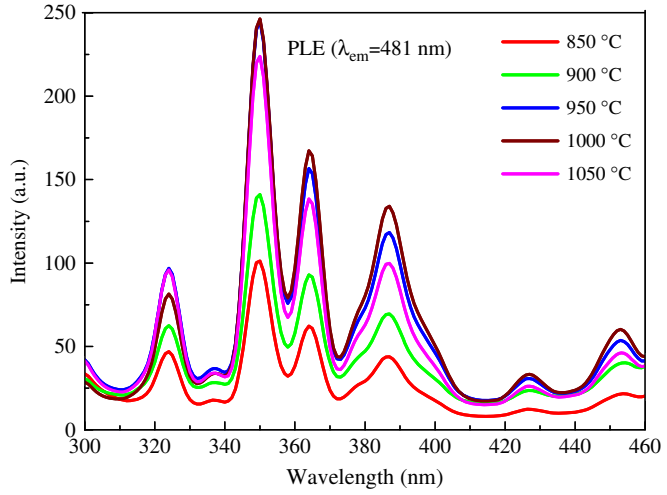

Fig. 3. The PLE spectra of $LiSr_{3.98}(BO_3)_3$:0.02Dy^{3+} phosphors (λ_{em}=481 nm).

3.2.2. PLE spectra

Fig. 3 shows the PLE spectra of $LiSr_{3.98}(BO_3)_3$:0.02Dy^{3+} phosphors monitored at 481 nm. The PLE spectra are very similar. The excitation spectra in the range 300–460 nm come from the ground state of $^6H_{15/2}$ to the excited states of $4f^9$ electronic configurations of the Dy^{3+} ions, which are located at 324 nm ($^6H_{15/2}\rightarrow{}^4M_{17/2}$), 350 nm ($^6H_{15/2}\rightarrow{}^6P_{7/2}$), 364 nm ($^6H_{15/2}\rightarrow{}^4I_{11/2}$), 388 nm ($^6H_{15/2}\rightarrow{}^4I_{13/2}$), 427 nm ($^6H_{15/2}\rightarrow{}^4G_{11/2}$) and 454 nm ($^6H_{15/2}\rightarrow{}^4I_{15/2}$) [24]. Among all the excitation bands, the band at 350 nm possesses the maximum intensity. The excitation band of $LiSr_{3.98}(BO_3)_3$:0.02Dy^{3+} phosphor matches well with the NUV emitting of InGaN chip, implying a potential application of the investigated phosphor in NUV-pumped w-LEDs.

3.2.3. PL spectra

Fig. 4 shows the PL emission spectra of $LiSr_{3.98}(BO_3)_3$:0.02Dy^{3+} phosphors at different temperatures. The

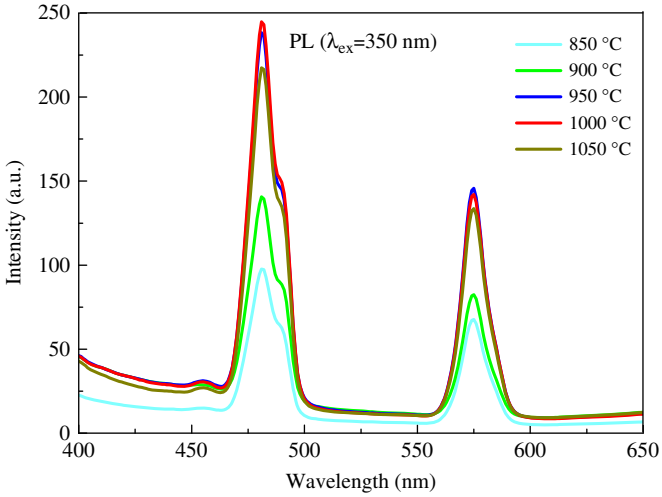

Fig. 4. The PL spectra of $LiSr_{3.98}(BO_3)_3$:0.02Dy^{3+} phosphors at different synthesis temperatures.

observed emission spectra exhibit two strong bands centered at 481 nm (blue) and 575 nm (yellow), which corresponded to $^4F_{9/2}\rightarrow{}^6H_{15/2}$ and $^4F_{9/2}\rightarrow{}^6H_{13/2}$ transitions, respectively. In addition, the position of emission peak is not changed with different synthesis temperature. It is well known that the $^4F_{9/2}\rightarrow{}^6H_{15/2}$ magnetic dipole transition is prominent when Dy^{3+} is located at high symmetry, while the $^4F_{9/2}\rightarrow{}^6H_{13/2}$ electric dipole transition is stronger when Dy^{3+} is located at low-symmetry sites [20]. In our case, the blue emission ($^4F_{9/2}\rightarrow{}^6H_{15/2}$) at 481 nm is stronger than the yellow emission ($^4F_{9/2}\rightarrow{}^6H_{13/2}$) at 575 nm, which illustrates that the Dy^{3+} ions occupy a high-symmetry site in the investigated $LiSr_4(BO_3)_3$ host. According to the crystal structure of $LiSr_4(BO_3)_3$ depicted in Fig. 1, it is confirmed that the Dy^{3+} ion prefers to replace the Sr^{2+} in the 16a position in the $LiSr_4(BO_3)_3$ compound.

With the increasing of the synthesis temperature, the PL intensity is accordingly enhanced. The strongest emission intensity of the $LiSr_{3.98}(BO_3)_3$:0.02Dy^{3+} phosphor synthesized at 1000 °C is remarkably enhanced by a factor of 2.5 with comparison to that at 850 °C. It is ascribed to the increasing of the crystalline size upon the raising temperature, which gives rise to a decreasing of light scattering. However, the samples tended to clump and agglomerate seriously when calcined at 1050 °C, and then the integrity of lattices was destroyed during the grinding process, which caused the emission intensity to decrease.

The energy levels of Dy^{3+} ions and visible emission are depicted in Fig. 5 according to the calculated data of energy levels by Carnall et al. [25,26]. When the 4*f* higher energy level of Dy^{3+} ions is excited by 350 nm n-UV light, the initial population relaxes to the lower energy levels until it arrives at the $^4F_{9/2}$ level by phonon-assisted process, then it gives rise to the blue and yellow light emission, as shown in Fig. 4.

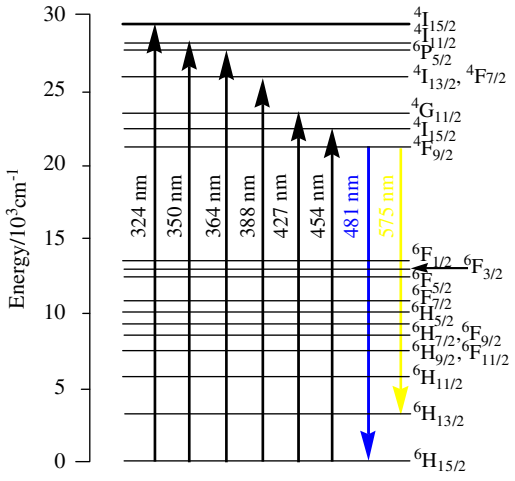

Fig. 5. The schematic energy levels of Dy^{3+}.

3.3. Luminescence properties for $LiSr_4(BO_3)_3:Dy^{3+}$ phosphors with different codopant concentration

Fig. 6(a) and (b) shows the excitation spectra (λ_{em}=481 nm) and emission spectra (λ_{ex}=350 nm) of $LiSr_4(BO_3)_3:Dy^{3+}$ phosphors with 0.5%, 1%, 1.5%, 2%, 3% and 6% of Dy^{3+} concentration. The emission intensity of the $^4F_{9/2} \rightarrow {}^6H_{15/2}$ transition under 350 nm excitation as a function of Dy^{3+} doping concentration (x value) increases rapidly with the increase of Dy^{3+} concentration, and reaches a maximum value at 2%, then decreases with increasing Dy^{3+} ions due to the concentration quenching as shown in the inset of Fig. 6(b).

The concentration quenching of the luminescence is due to the energy transfer from one activator to another until all energy is consumed. For this reason, it is necessary to obtain the critical distance (R_c), that is, the critical separation between donor (activators) and acceptors (quenching site). The critical distance R_c of the energy transfer between the same activators Dy^{3+} in the $LiSr_4(BO_3)_3:Dy^{3+}$ phosphors can be estimated according to the following equation [27]:

$$R_c = 2\left(\frac{3V}{4\pi x_c N}\right)^{\frac{1}{3}} \quad (1)$$

where x_c is the critical concentration, N is the number of the Sr^{2+} ions in the unit cell and V is the volume of the unit cell. By taking the experimental and analytic values of x_c, N and V (0.02, 64 and 3341.80 Å^3, respectively), the critical transfer distance of Dy^{3+} in $LiSr_{4-x}(BO_3)_3:xDy^{3+}$ phosphors is found to be about 17.09 Å

3.4. The mechanism of the energy transfer among Dy^{3+} ions

According to Huang's rule [28], the relationship between the integral luminescent intensity I and doping concentration x can be expressed as follows:

$$I \propto \alpha^{(1-\frac{s}{d})}\Gamma\left(1+\frac{s}{d}\right) \quad (2)$$

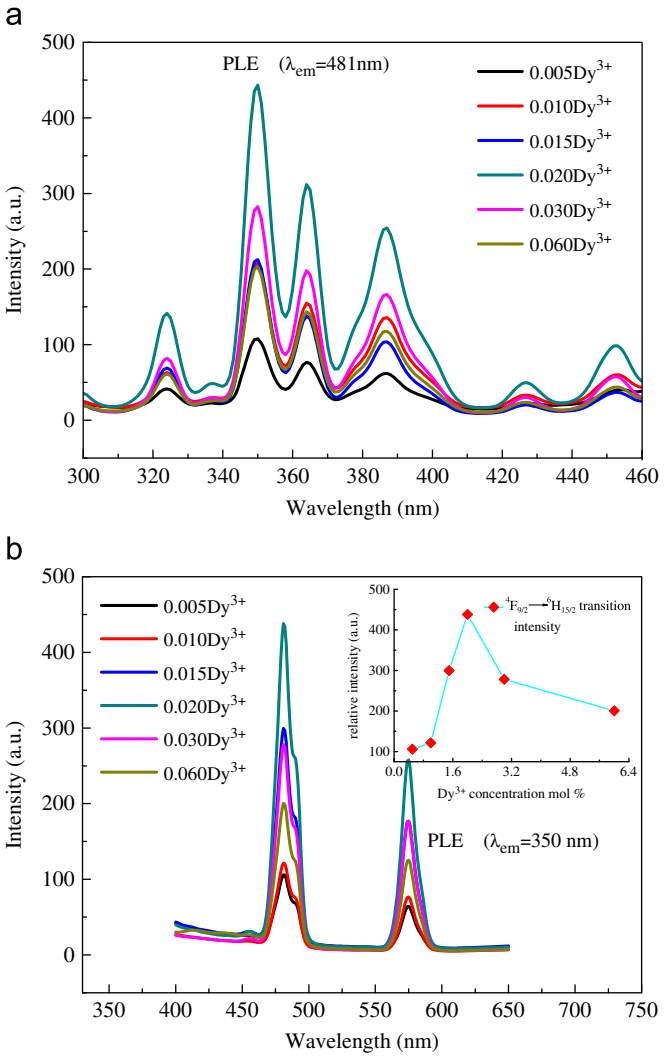

Fig. 6. (a) The PLE spectra of $LiSr_{4-x}(BO_3)_3:xDy^{3+}$ phosphors (λ_{em}=481 nm). (b). The PL spectra of $LiSr_{4-x}(BO_3)_3:xDy^{3+}$ phosphors under 350 nm excitation.

$$\alpha = x\Gamma\left(1-\frac{d}{s}\right)\left[X_0\frac{1+A}{\gamma}\right]^{\frac{d}{s}} \quad (3)$$

where γ is the intrinsic transition probability of sensitizer, s is index of electric multipole, which is six, eight and ten for electric dipole–dipole, electric dipole–quadrupole, and electric quadrupole–quadrupole interaction, respectively. If s=3, the interaction type is an exchange interaction. d is the dimension of the sample, here d=3. A and X_0 are the constants and $\Gamma(1+s/d)$ is a function. From Eqs. (2) and (3), it can be derived that

$$\log\left(\frac{I}{x}\right) = -\frac{s}{d}\log x + \log f \quad (4)$$

where f is independent of the doping concentration. Fig. 7 shows the $\log(I/x) - \log x$ plot for the $^4F_{9/2} \rightarrow {}^6H_{15/2}$ transitions of Dy^{3+} ions in $LiSr_{4-x}(BO_3)_3:xDy^{3+}$ phosphors. According to Eq. (4), using linear fitting to deal with the experimental data in the region of high

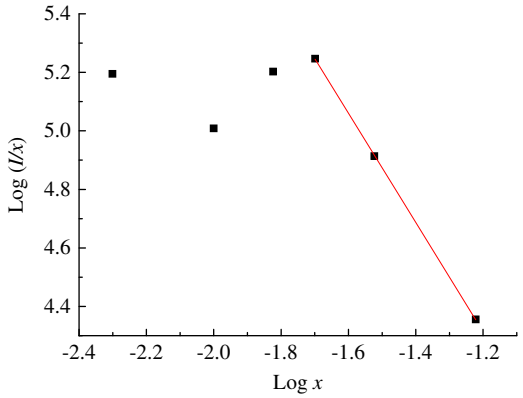

Fig. 7. The relation of the concentration of Dy^{3+} ions log (x)and the log (I/x) for the $^4F_{9/2}\rightarrow{}^6H_{13/2}$ transition by 350 nm light.

concentrations, the value of the slope parameter $-s/d$ is obtained to be -1.87 for the $^4F_{9/2}\rightarrow{}^6H_{15/2}$ transition. The slope parameter is approximately -2. Therefore, the index of the electric multipole energy transfer is 6. The result means that the electric dipole–dipole interaction mechanism is dominant by the energy transfer of the Dy^{3+} ions in the investigated phosphors.

3.5. Simulation of white light emission from $LiSr_{4-x}(BO_3)_3{:}xDy^{3+}$ phosphors

Generally, the relative intensity ratio of the yellow (575 nm) to blue (481 nm) emission can be used to examine the structural distortion around Dy^{3+} ions. The values of Y/B ratio in the $LiSr_{4-x}(BO_3)_3{:}xDy^{3+}$ are 0.59, 0.59, 0.59, 0.61, 0.63 and 0.63 corresponding to 0.5%, 1%, 1.5%, 2%, 3% and 6% Dy^{3+}-doped concentration, respectively. The results imply that the distortion of Dy^{3+} ions located in the crystal lattices increase with increasing the Dy^{3+} concentration due to the substitution of smaller Dy^{3+} ions (1.027 Å, $CN=8$) for the larger Sr^{2+} ions (1.26 Å, $CN=8$) in $LiSr_4(BO_3)_3$. The variation of Y/B intensity ratios indicates the feasibility of the generation of white light in the investigated phosphors.

Color coordinate is an important parameter for phosphors in white LED application. The CIE chromaticity coordinates of $LiSr_{4-x}(BO_3)_3{:}xDy^{3+}$ phosphors with different Dy^{3+} concentrations were calculated from the emission spectra (Fig. 6b) and presented in Fig. 8. The dot ∗ in CIE-1931 chromaticity diagram shows the ideal white light chromaticity coordinates with $x=0.333$ and $y=0.333$. Generally, the closer the CIE chromaticity coordinates to dot ∗, the higher the white-light-emitting quality. The chromaticity coordinates of $LiSr_{4-x}(BO_3)_3{:}xDy^{3+}$ phosphors moved toward the ideal white light coordinates (0.333 and 0.333) with increasing Dy^{3+} content. The CIE values for 0.5%, 1%, 1.5%, 2%, 3% and 6% Dy^{3+}-doped concentrations were as following A ($x=0.261$, $y=0.264$), B ($x=0.266$, $y=0.279$), C ($x=0.266$, $y=0.291$), D ($x=0.269$, $y=0.303$), E ($x=0.273$, $y=0.303$) and F ($x=0.261$, $y=0.275$), respectively. The tunable white luminescence in the $LiSr_{4-x}(BO_3)_3{:}xDy^{3+}$ phosphors could

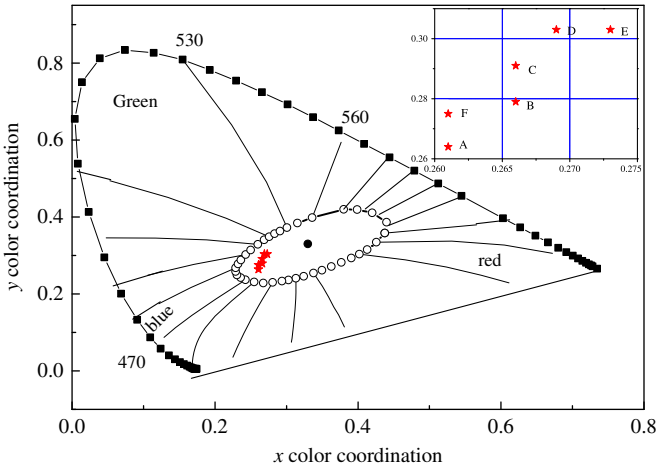

Fig. 8. CIE coordinate diagram of $LiSr_{4-x}(BO_3)_3{:}xDy^{3+}$ phosphors by 350 nm light.

be obtained by adjusting the yellow to blue intensity ratio based on the Dy^{3+} concentration. The CIE chromaticity coordinates for $LiSr_{4-x}(BO_3)_3{:}xDy^{3+}$ phosphors located in the bluish-white region. Indeed, it is worth researching further to improve the orange–red emission in $LiSr_{4-x}(BO_3)_3{:}xDy^{3+}$.

4. Conclusions

In summary, $LiSr_{4-x}(BO_3)_3{:}xDy^{3+}$, as a single phase full color phosphor, was synthesized successfully by a solid-state reaction. The study presented that the $LiSr_{4-x}(BO_3)_3{:}xDy^{3+}$ could be excited by near-ultraviolet (NUV) light in the region 300–460 nm and the emission peaks located at 481 nm (blue) and 575 nm (yellow). The critical transfer distance of Dy^{3+} in $LiSr_{4-x}(BO_3)_3{:}xDy^{3+}$ phosphors is about 17.09 Å. The CIE chromaticity coordinates for $LiSr_{4-x}(BO_3)_3{:}xDy^{3+}$ phosphors located in the yellowish-white region. These results indicate that this $LiSr_{4-x}(BO_3)_3{:}xDy^{3+}$ phosphors show potential application in NUV white LED to be free of complicated phosphor blending operation.

Acknowledgments

We gratefully acknowledge financial support by the National Natural Science Foundation of China (no. 11165010) and the Foundation of Qinhuangdao Science and Technology Board in China (no. 201101A023). We also gratefully acknowledge instrumental analysis center of Hebei Normal University of Science and Technology.

References

[1] A. Bergh, G. Craford, A. Duggal, R. Haitz, The promise and challenge of solid-state lighting, Physics Today 54 (2001) 42–47.
[2] A.H. Narendran, M.A. Petruska, M. Achermann, D.J. Weeder, E.A. Akhadov, D.D. Koleske, M.A. Hoffbauer, V.I. Klimov, Multi-color light-emitting diodes based on semiconductor nanocrystals

encapsulated in GaN charge injection layers, Nano Letters 5 (2005) 1039–1044.
[3] A. Kitai, Luminescent Materials and Application, John Wiley & Sons, Ltd., 2008 P75.
[4] S. Choi, Y. Young, H. Jung, Eu^{2+} and Mn^{2+} activated single phase white emitting phosphor Na(Sr,Ba)PO_4 for phosphor converted-LEDs, Materials Letters 75 (2012) 186–188.
[5] G. Li, D. Geng, M. Shang, Y. Zhang, C. Peng, Z. Chong, J. Lin, Color tuning luminescence of $Ce^{3+}/Mn^{2+}/Tb^{3+}$-triactivated $Mg_2Y_8(SiO_4)6O_2$ via energy transfer: potential single-phase white-light-emitting phosphors, Journal of Physical Chemistry C 115 (2011) 21882–21892.
[6] P. Li, Z. Wang, Z. Yang, Q. Guo, $Sr_2B_2P_2O_{10}$:Eu^{2+},Mn^{2+},Ba^{2+}: a potential single-phase white light-emitting phosphor for UV light emitting diodes, Journal of the Electrochemical Society 157 (2010) H504–H509.
[7] J.S. Kim, P.E. Jeon, J.C. Choi, H.L. Park, Warm-white-light emitting diode utilizing a single-phase full-color $Ba_3MgSi_2O_8$:Eu^{2+}, Mn^{2+} phosphor, Applied Physics Letters 84 (2004) 2931–2933.
[8] B. Liu, Y. Wang, J. Zhou, F. Zhang, Z. Wang, The reduction of Eu^{3+} to Eu^{2+} in $BaMgAl_{10}O_{17}$:Eu and the photoluminescence properties of $BaMgAl_{10}O_{17}$:Eu^{2+} phosphor, Journal of Applied Physics 106 (2009) 1–5 053102.
[9] B.V. Ratnam, M. Jayasimhadri, K. Jang, H.S. Lee, S.S. Yi, J.H. Jeong, White light emission from $NaCaPO_4$:Dy^{3+} phosphor for ultraviolet-based white light-emitting diodes, Journal of the American Ceramic Society 93 (2010) 3857–3861.
[10] M. Peng, Z. Pei, G. Hong, Q. Su, The reduction of Eu^{3+} to Eu^{2+} in $BaMgSiO_4$:Eu prepared in air and the luminescence of $BaMgSiO_4$:Eu^{2+} phosphor, Journal of Materials Chemistry 13 (2003) 1202–1205.
[11] C. Huang, T. Chen, A Novel Single-Composition, Trichromatic white-light $Ca_3Y(GaO)_3(BO_3)_4$:Ce^{3+}, Mn^{2+}, Tb^{3+} phosphor for UV-light emitting diodes, The Journal of Chemical Physics 115 (2011) 2349–2355.
[12] Y. Liu, Z. Yang, Q. Yu, X. Li, Y. Yang, P. Li, Luminescence properties of $Ba_2LiB_5O_{10}$:Dy^{3+} phosphor, Materials Letters 65 (2011) 1956–1958.
[13] R. Zhang, X. Wang, Preparation and luminescent characteristics of $Sr_3RE_2(BO_3)_4$:Dy^{3+} (*RE*=Y, La, Gd) phosphors for white LED, Journal of Alloys and Compounds 509 (2011) 1197–1200.
[14] L. Wu, X. Chen, H. Li, M. He, Y. Xu, X. Li, Structure determination and relative properties of novel cubic borates $MM'_4(BO_3)_3$ (M=Li, Na, K; M'=Ca, Sr, Ba), Inorganic Chemistry 44 (2005) 6409–6414.
[15] C. Guo, X. Ding, H.J. Seo, Z. Ren, J. Bai, Double emitting phosphor $NaSr_4(BO_3)_3$:Ce^{3+}, Tb^{3+} for near-UV light-emitting diodes, Optics and Laser Technology 43 (2011) 1351–1354.
[16] L. Jiang, Y. Zhang, C. Li, J. Hao, Q. Su, Thermoluminescence properties of Ce^{3+}-doped $LiSr_4(BO_3)_3$ phosphor, Materials Letters 61 (2007) 5107–5109.
[17] X. Zhang, H.J. Seo, Photoluminescence and concentration quenching of $NaCa_4(BO_3)_3$:Eu^{3+} phosphor, Journal of Alloys and Compounds 503 (2010) L14–L17.
[18] X. Zhang, H. Lang, H.J. Seo, On the luminescence of Ce^{3+}, Eu^{3+}, and Tb^{3+} in novel borate $LiSr_4(BO_3)_3$, Journal of Fluorescence 21 (2011) 1111–1115.
[19] J. Sun, X. Zhang, Z. Xia, H. Du, Synthesis and luminescence properties of novel $LiSrPO_4$:Dy^{3+} phosphor, Materials Research Bulletin 46 (2011) 2179–2182.
[20] B. Liu, C. Shi, Z. Qi, Potential white-light long-lasting phosphor:Dy^{3+}-doped aluminate, Applied Physics Letters 86 (2005) 1–3 191111.
[21] Q. Wang, D. Deng, Y. Hua, L. Huang, H. Wang, S. Zhao, G. Jia, C. Li, S. Xu, Potential tunable white-emitting phosphor $LiSr_4(BO_3)_3$:Ce^{3+}, Eu^{2+} for ultraviolet light-emitting diodes, Journal of Luminescence 132 (2012) 434–438.
[22] X. Sun, L. Lin, W. Wang, J. Zhang, White-light emission from $Li_2Sr_{1-3x/2}Dy_xSiO_4$ Phosphors, Applied Physics A 104 (2011) 83–88.
[23] S.H. Jung, D.S. Kang, D.Y. Jeon, Effect of substitution of nitrogen ions to red-emitting $Sr_3B_2O_{6-3/2x}N_x$:Eu^{2+} oxy-nitride phosphor for the application to white LED, Journal of crystal growth 326 (2011) 116–119.
[24] P. You, G. Yin, X. Chen, B. Yue, Z. Huang, X. Liao, Y. Yao, Luminescence properties of Dy^{3+}-doped Li_2SrSiO_4 for NUV-excited white LEDs, Optical Materials 33 (2011) 1808–1812.
[25] X. Sun, J. Zhang, X. Liu, L. Lin, Enhanced luminescence of novel $Ca_3B_2O_6$:Dy^{3+} phosphors by Li^+-codoping for LED applications, Ceramics International 38 (2012) 1065–1070.
[26] W.T. Carnall, P.R. Fields, K. Rajnak, Electronic energy levels in the trivalent lanthanide aquo ions. I. Pr^{3+}, Nd^{3+}, Pm^{3+}, Sm^{3+}, Dy^{3+}, Ho^{3+}, Er^{3+}, and Tm^3, The Journal of Chemical Physics 49 (1968) 4424–4442.
[27] G. Blasse, Energy transfer in oxides phosphors, Philips Research Reports 24 (1969) 131–136.
[28] G. Li, D. Geng, M. Shang, Y. Zhang, C. Peng, Z. Chong, J. Lin, Color tuning luminescence of $Ce^{3+}/Mn^{2+}/Tb^{3+}$-triactivated $Mg_2Y_8(SiO_4)_6O_2$ via energy transfer: potential single-phase white-light-emitting phosphors, Journal of Physical Chemistry C 115 (2011) 21882–21892.